

Extended Higgs Sectors Beyond the Standard Model

WINTER SEMESTER 2018/19

KARLSRUHE INSTITUTE OF TECHNOLOGY (KIT)

LECTURE GIVEN BY

PROF. DR. M. M. MÜHLEITNER

Contents

1	The Standard Model Higgs Sector	1
1.1	The Introduction of the Higgs Boson	1
1.2	The Standard Model Higgs sector	3
1.3	Verification of the Higgs mechanism	5
1.4	Higgs boson decays	5
1.5	Higgs boson production at the LHC	9
1.6	Higgs Boson Discovery	13
1.7	Higgs boson couplings at the LHC	14
1.8	Higgs Boson Quantum Numbers	16
1.9	Determination of the Higgs self-interactions	20
1.9.1	Determination of the Higgs self-couplings at the LHC	20
1.10	Summary	22
2	Appendix	25
2.1	Beispiel: Feldtheorie für ein komplexes Feld	25
	Bibliography	26

Preliminary Content

This lecture will discuss Higgs sectors of various extensions beyond the Standard Model.

1. Revision of the Standard Model (SM) Higgs Sector
2. 2 Higgs Doublet Model
3. The Minimal Supersymmetric Extension of the SM (MSSM)
4. The Next-to-Minimal Supersymmetric Extension of the SM (NMSSM)
5. Composite Higgs Model

Chapter 1

The Standard Model Higgs Sector

Literature:

1. Recent physics results are presented on the webpages of the LHC experiments ATLAS and CMS.
2. A. Djouadi, “The Anatomy of electro-weak symmetry breaking. I: The Higgs boson in the standard model,” *Phys. Rept.* **457** (2008) 1 [hep-ph/0503172].
3. M. Spira, “QCD effects in Higgs physics,” *Fortsch. Phys.* **46** (1998) 203 [hep-ph/9705337] and “Higgs Boson Production and Decay at Hadron Colliders”, *Prog. Part. Nucl. Phys.* **95** (2017) 98.
4. S. Dittmaier *et al.* [LHC Higgs Cross Section Working Group Collaboration], “Handbook of LHC Higgs Cross Sections: 1. Inclusive Observables,” arXiv:1101.0593 [hep-ph].
5. S. Dittmaier, S. Dittmaier, C. Mariotti, G. Passarino, R. Tanaka, S. Alekhin, J. Alwall and E. A. Bagnaschi *et al.*, “Handbook of LHC Higgs Cross Sections: 2. Differential Distributions,” arXiv:1201.3084 [hep-ph].
6. S. Heinemeyer *et al.* [LHC Higgs Cross Section Working Group Collaboration], “Handbook of LHC Higgs Cross Sections: 3. Higgs Properties,” arXiv:1307.1347 [hep-ph].
7. De Florian *et al.*, “Handbook of LHC Higgs Cross Sections: 4. Deciphering the Nature of the Higgs Sector,” arXiv:1610.07922 [hep-ph].
8. H. E. Logan, “TASI 2013 lectures on Higgs physics within and beyond the Standard Model,” arXiv:1406.1786 [hep-ph].
9. Some material on the SM Higgs sector can also be found in my lectures TTP1 and TTP2 and in my lectures on supersymmetry at colliders.

1.1 The Introduction of the Higgs Boson

There are two reasons for the introduction of the Higgs boson [1, 2] in the Standard Model (SM) of particle physics:

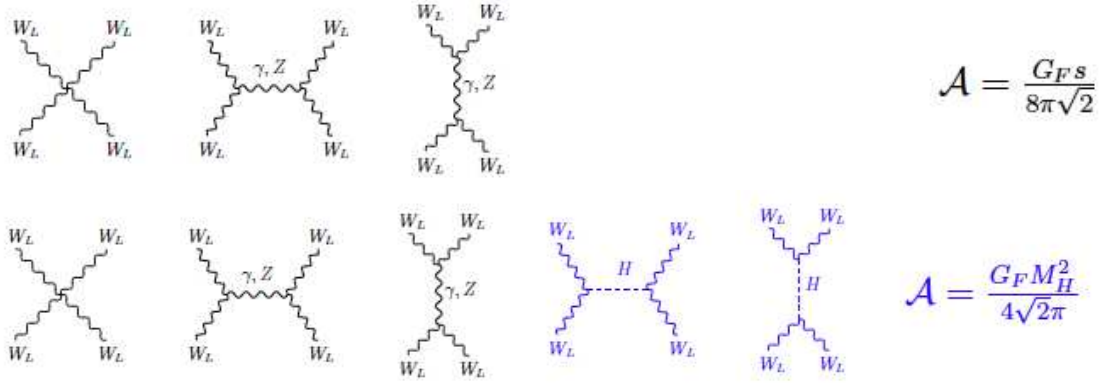


Figure 1.1: The scattering of longitudinal gauge bosons in longitudinal gauge bosons. Upper: without a Higgs boson. Lower: with a Higgs boson

1. A theory of massive gauge bosons and fermions, which is weakly interacting up to very high energies, requires for unitarity reasons the existence of a Higgs particle. The Higgs particle is a scalar 0^+ particle, *i.e.* a spin 0 particle with positive parity, which couples to the other particles with a coupling strength proportional to the mass (squared) of the particles.

Look *e.g.* at the amplitude for the scattering of longitudinal gauge bosons W_L into a pair of longitudinal gauge bosons W_L , see Fig. 1.1. Without a Higgs boson the amplitude diverges proportional to the center-of-mass (c.m) energy squared, s , *cf.* Fig. 1.1 (upper), where G_F denotes the Fermi constant. The introduction of a Higgs boson which couples proportional to the mass squared of the gauge boson, regularizes the amplitude, *cf.* Fig. 1.1 (lower), where M_H denotes the Higgs boson mass.

2. The introduction of mass terms for the gauge bosons violates the $SU(2)_L \times U(1)$ symmetry of the SM Lagrangian. The same problem arises for the introduction of mass terms for the fermions. It violates the chiral symmetry.

Let us have a closer look at point 2. We look at the Lagrangian

$$\mathcal{L}_f = \bar{\Psi}(i\gamma^\mu D_\mu - m)\Psi . \quad (1.1)$$

In the chiral representation the 4×4 γ matrices are given by

$$\gamma^\mu = \left(\left(\begin{array}{cc} \mathbf{0} & \mathbf{1} \\ \mathbf{1} & \mathbf{0} \end{array} \right), \left(\begin{array}{cc} \mathbf{0} & -\vec{\sigma} \\ \vec{\sigma} & \mathbf{0} \end{array} \right) \right) = \left(\begin{array}{cc} 0 & \sigma_-^\mu \\ \sigma_+^\mu & 0 \end{array} \right) \quad (1.2)$$

$$\gamma^5 = \left(\begin{array}{cc} \mathbf{1} & \mathbf{0} \\ \mathbf{0} & -\mathbf{1} \end{array} \right) , \quad (1.3)$$

where σ_i ($i = 1, 2, 3$) are the Pauli matrices. With

$$\Psi = \begin{pmatrix} \chi \\ \varphi \end{pmatrix} \quad \text{and} \quad \bar{\Psi} = \Psi^\dagger \gamma^0 = (\chi^\dagger, \varphi^\dagger) \begin{pmatrix} 0 & \mathbf{1} \\ \mathbf{1} & 0 \end{pmatrix} = (\varphi^\dagger, \chi^\dagger) \quad (1.4)$$

we get

$$\bar{\Psi} i \gamma^\mu D_\mu \Psi = i(\varphi^\dagger, \chi^\dagger) \underbrace{\begin{pmatrix} 0 & \sigma_-^\mu \\ \sigma_+^\mu & 0 \end{pmatrix}}_{\begin{pmatrix} \sigma_-^\mu D_\mu \varphi \\ \sigma_+^\mu D_\mu \chi \end{pmatrix}} \begin{pmatrix} D_\mu \chi \\ D_\mu \varphi \end{pmatrix} = \varphi^\dagger i \sigma_-^\mu D_\mu \varphi + \chi^\dagger i \sigma_+^\mu D_\mu \chi. \quad (1.5)$$

The gauge interaction¹ holds independently for

$$\Psi_L = \begin{pmatrix} 0 \\ \varphi \end{pmatrix} = \frac{1}{2}(\mathbb{1} - \gamma_5)\Psi \quad \text{and} \quad \Psi_R = \begin{pmatrix} \chi \\ 0 \end{pmatrix} = \frac{1}{2}(\mathbb{1} + \gamma_5)\Psi. \quad (1.6)$$

The Ψ_L and Ψ_R can transform differently under gauge transformations,

$$\Psi'_L = U_L \Psi_L \quad \text{and} \quad \Psi'_R = U_R \Psi_R. \quad (1.7)$$

But

$$m \bar{\Psi} \Psi = m(\varphi^\dagger, \chi^\dagger) \begin{pmatrix} \chi \\ \varphi \end{pmatrix} = m(\varphi^\dagger \chi + \chi^\dagger \varphi) = m(\bar{\Psi}_L \Psi_R + \bar{\Psi}_R \Psi_L). \quad (1.8)$$

The mass term mixes Ψ_L and Ψ_R . From this follows *symmetry breaking* if Ψ_L and Ψ_R transform differently.

What about the mass term for gauge bosons? We have the Lagrangian

$$\mathcal{L} = -\frac{1}{4} \underbrace{F^{\alpha\mu\nu} F_{\mu\nu}^a}_{\text{gauge invariant}} + \frac{m^2}{2} \underbrace{A^{a\mu} A_\mu^a}_{\text{not gauge invariant}}. \quad (1.9)$$

For example for the $U(1)$ we get²

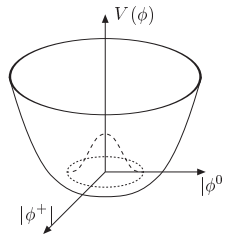
$$(A_\mu A^\mu)' = (A_\mu + \partial_\mu \theta)(A^\mu + \partial^\mu \theta) = A_\mu A^\mu + 2A_\mu \partial^\mu \theta + (\partial_\mu \theta)(\partial^\mu \theta). \quad (1.10)$$

The mass term A^μ breaks the gauge symmetry.

1.2 The Standard Model Higgs sector

The problem of mass generation without violating gauge symmetries can be solved by introducing an $SU(2)_L$ Higgs doublet³ with weak isospin $I = 1/2$ and hypercharge $Y = 1$ and the SM Higgs potential given by

$$V(\Phi) = \lambda \left[\Phi^\dagger \Phi - \frac{v^2}{2} \right]^2. \quad (1.11)$$



¹Question: What is the gauge principle?

²The kinetic Lagrangian $-1/4 F_{\mu\nu} F^{\mu\nu}$ is invariant under a gauge transformation $A_\mu \rightarrow A'_\mu = A_\mu + \partial_\mu \theta$.

³Question: Why do we need to introduce a doublet?

Here v denotes the vacuum expectation value (VEV)

$$v = \frac{1}{\sqrt{\sqrt{G_F}}} \approx 246.22 \text{ GeV}, \quad (1.12)$$

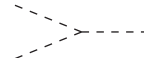
and $G_F = 1.16637 \cdot 10^{-5} \text{ GeV}^{-2}$ the Fermi constant. Introducing the Higgs field in a physical gauge,

$$\Phi = \frac{1}{\sqrt{2}} \begin{pmatrix} 0 \\ v + H \end{pmatrix}, \quad (1.13)$$

the Higgs potential can be written as

$$V(H) = \frac{1}{2} M_H^2 H^2 + \frac{M_H^2}{2v} H^3 + \frac{M_H^2}{8v^2} H^4. \quad (1.14)$$

Here we can read off directly the mass of the Higgs boson and the Higgs trilinear and quartic self-interactions. Adding the couplings to gauge bosons and fermions we have⁴:

Mass of the Higgs boson	$M_H = \sqrt{2\lambda}v$	
Couplings to gauge bosons	$g_{VVH} = \frac{2M_V^2}{v}$	
Yukawa couplings	$g_{ffH} = \frac{m_f}{v}$	
Trilinear coupling [units $\lambda_0 = 33.8 \text{ GeV}$]	$\lambda_{HHH} = 3\frac{M_H^2}{M_Z^2}$	
Quartic coupling [units λ_0^2]	$\lambda_{HHHH} = 3\frac{M_H^2}{M_Z^4}$	

In the SM the trilinear and quartic Higgs self-couplings are uniquely determined by the mass of the Higgs boson. As can be read off from the table, before the Higgs discovery the only unknown parameter was the Higgs boson mass.

The Higgs potential with its typical form leads to a non-vanishing VEV v in the ground state. Expansion of Φ around the minimum of the Higgs potential leads to one massive scalar particle, the Higgs boson, and three massless Goldstone bosons, that are absorbed to give masses to the charged W bosons and the Z boson. (For a toy example, see Appendix 2.1.) The appearance of Goldstone bosons is stated in the Goldstone theorem, which says:

Be

- N = dimension of the algebra of the symmetry group of the complete Lagrangian.
- M = dimension of the algebra of the group, under which the vacuum is invariant after spontaneous symmetry breaking.

\Rightarrow There are $N - M$ Goldstone bosons without mass in the theory.

The Goldstone theorem states that for each spontaneously broken degree of freedom of the symmetry there is one massless Goldstone boson.

In gauge theories, however, the conditions for the Goldstone theorem are not fulfilled: Massless scalar degrees of freedom are absorbed by the gauge bosons to give them mass. The Goldstone phenomenon leads to the Higgs phenomenon.

⁴The trilinear and quartic Higgs self-couplings are given in terms of $\lambda_0 = M_Z^2/v \approx 33.8 \text{ GeV}$.

1.3 Verification of the Higgs mechanism

On 4th July 2012, the LHC experiments ATLAS and CMS announced the discovery of a new scalar particle with mass $M_H \approx 125$ GeV [3, 4]. The discovery triggered immediately the investigation of the properties of this particle in order to test if it is indeed the Higgs particle that has been discovered. In order to verify experimentally the Higgs mechanism as the mechanism that allows to generate particle masses without violating gauge principles, we have to perform several steps:

- 1.) First of all the Higgs particle has to be discovered.
- 2.) In the next step its couplings to gauge bosons and fermions are measured. If the Higgs mechanism acts in nature these couplings are proportional to the masses (squared) of the respective particles.
- 3.) Its spin and parity quantum numbers have to be determined.
- 4.) And finally, the Higgs trilinear and quartic self-couplings must be measured. This way, the Higgs potential can be reconstructed which, with its typical minimax form, is responsible for the non-vanishing vacuum expectation value, that is essential for the non-zero particle masses.

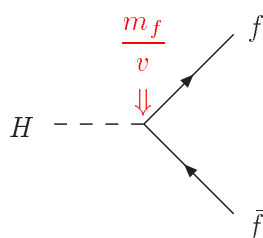
In the following, we will see how this program can be performed at the LHC.

1.4 Higgs boson decays

In order to search for the Higgs boson at existing and future colliders, one has to know what to look for. Hence, one has to study the Higgs decay channels. Since the Higgs boson couples proportional to the mass of the particle its preferred decays will be those into heavy particles, *i.e.* heavy fermions and, when kinematically allowed, into gauge bosons. The branching ratio into a final state pair XX is defined as

$$\text{BR}(H \rightarrow XX) = \frac{\Gamma(H \rightarrow XX)}{\Gamma_{\text{tot}}^H}. \quad (1.15)$$

The partial decay width for the decay $H \rightarrow XX$ is given by $\Gamma(H \rightarrow XX)$. The total decay width Γ_{tot}^H is the sum of all possible partial decay widths of H . All possible branching ratios hence have to add up to 1. For the SM Higgs boson of mass $M_H = 125.09$ GeV the branching ratios into fermions are



$$\begin{aligned}
BR(H \rightarrow b\bar{b}) &\lesssim 0.5797 \\
BR(H \rightarrow \tau^+\tau^-) &\lesssim 0.06244 \\
BR(H \rightarrow c\bar{c}) &\lesssim 0.02879 \\
BR(H \rightarrow t\bar{t}) &\lesssim 0 \quad (\text{kinematically closed})
\end{aligned} \tag{1.16}$$

These and the following branching ratios are obtained from the program `HDECAY` [5, 6]. It is a Fortran code for the computation of the branching ratios and total widths of the SM Higgs boson and also of the MSSM and 2HDM Higgs bosons. The decay widths include, where applicable, the state-of-the-art higher-order QCD and electroweak corrections. Furthermore, off-shell decays into heavy-quark, massive gauge boson, neutral Higgs pair as well as Higgs and gauge boson final states. The latter two decays do not exist in the SM Higgs sector but only in extended Higgs sectors with a larger Higgs spectrum. There are also other programs on the market for the computation of the SM Higgs decays, see [7, 8, 9] for an overview.

The tree-level partial decay width into fermions is given by

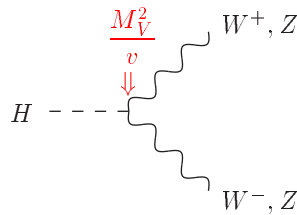
$$\Gamma(H \rightarrow f\bar{f}) = \frac{N_{cf}G_F M_H}{4\sqrt{2}\pi} m_f^2 \beta^3, \tag{1.17}$$

with the velocity

$$\beta = (1 - 4m_f^2/M_H^2)^{1/2} \tag{1.18}$$

of the fermions, their mass m_f , and the colour factor $N_{cf} = 1(3)$ for leptons (quarks). The decays into quark pair final states receive large QCD corrections which have been calculated by various groups and can amount up to -50%. [Braaten, Leveille; Sakai; Inami, Kubota; Drees, Hikasa; Gorishnii, Kataev, Larin, Surguladze; Kataev, Kim; Larin, van Ritbergen, Vermaseren; Chetyrkin, Kwiatkowski; Baikov, Chetyrkin, Kühn] - for details, see []].

For the SM Higgs boson with a mass of 125.09 GeV the branching ratios into gauge bosons are



$$\begin{aligned}
BR(H \rightarrow W^+W^-) &\lesssim 0.2167 \\
BR(H \rightarrow ZZ) &\lesssim 0.02657
\end{aligned} \tag{1.19}$$

For the 125 GeV Higgs boson these decays are off-shell, hence given by $H \rightarrow V^*V^* \rightarrow (f\bar{f})(f'\bar{f}')$ ($V = W, Z$). The Higgs boson decays into a pair of virtual vector bosons that subsequently decay into fermion pairs.

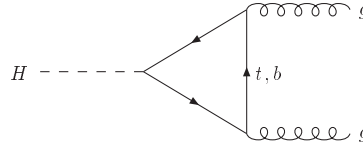
The formula for the tree-level decay width into a pair of on-shell massive gauge bosons $V = Z, W$ is given by

$$\Gamma(H \rightarrow VV) = \delta_V \frac{G_F M_H^3}{16\sqrt{2}\pi} \beta(1 - 4x + 12x^2), \tag{1.20}$$

with $x = M_V^2/M_H^2$, $\beta = \sqrt{1-4x}$ and $\delta_V = 2(1)$ for $V = W(Z)$. The electroweak corrections to these decays are of the order 5-20%.

[Fleischer, Jegerlehner; Bardin, ...; Kniehl; Ghinculov; Frink, ...] For a Higgs boson of mass $M_H = 125$ GeV off-shell decays $H \rightarrow V^*V^* \rightarrow 4l$ are important. The program PROPHECY4F includes the complete QCD and EW next-to-leading order (NLO) corrections to $H \rightarrow W^*W^*/Z^*Z^* \rightarrow 4f$ [Bredenstein, Denner; Dittmaier, Mück, Weber].

The decay into gluon pairs proceeds via a loop with the dominant contributions from top and bottom quarks:



For $M_H = 125.09$ GeV the branching ratio amounts to

$$BR(H \rightarrow gg) = 0.08157 . \quad (1.21)$$

At leading order (LO) the decay width can be cast into the form

$$\Gamma_{LO}(H \rightarrow gg) = \frac{G_F \alpha_s^2 M_H^3}{36\sqrt{2}\pi^3} \left| \sum_{Q=t,b} A_Q^H(\tau_Q) \right|^2 , \quad (1.22)$$

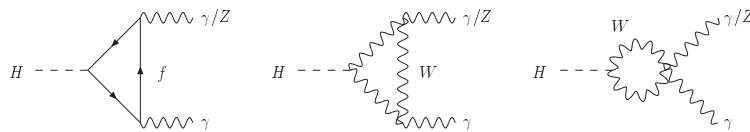
with the form factor

$$A_Q^H = \frac{3}{2}\tau[1 + (1 - \tau)f(\tau)] \quad (1.23)$$

$$f(\tau) = \begin{cases} \arcsin^2 \frac{1}{\sqrt{\tau}} & \tau \geq 1 \\ -\frac{1}{4} \left[\log \frac{1+\sqrt{1-\tau}}{1-\sqrt{1-\tau}} - i\pi \right]^2 & \tau < 1 \end{cases} . \quad (1.24)$$

The parameter $\tau_Q = 4M_Q^2/M_H^2$ is defined by the pole mass M_Q of the heavy quark Q in the loop. Note that for large quark masses the form factor approaches unity. The strong coupling constant is denoted by α_s . The QCD corrections have been calculated [Baikov, Chetyrkin; Chetyrkin, Kniehl, Steinhauser; Krämer, Laenen, Spira; Schröder, Steinhauser; Chetyrkin, Kühn, Sturm; Inami eal; Djouadi, Graudenz, Spira, Zerwas; Dawson eal; Harlander, Steinhauser; Harlander, Hofmann]. They are large and increase the branching ratio by about 70% at next-to-leading order (NLO). They are known at NLO including the full quark mass dependence and up to next-to-next-to-next-to leading order (N³LO) in the heavy top quark limit.

Further loop-mediated decays are those into 2 photons and a photon and a Z boson. They are mediated by charged fermion and W boson loops, the latter being dominant.



Although they amount only up to

$$BR(H \rightarrow \gamma\gamma) = 2.265 \times 10^{-3} \quad \text{and} \quad BR(H \rightarrow Z\gamma) = 1.537 \times 10^{-3} , \quad (1.25)$$

the $\gamma\gamma$ final state is an important search mode for light Higgs bosons at the LHC. The partial decay width into photons reads

$$\Gamma(H \rightarrow \gamma\gamma) = \frac{G_F \alpha^2 M_H^3}{128 \sqrt{2} \pi^3} \left| \sum_f N_{cf} e_f^2 A_f^H(\tau_f) + A_W^H(\tau_W) \right|^2, \quad (1.26)$$

with the form factors

$$A_f^H(\tau) = 2\tau[1 + (1 - \tau)f(\tau)] \quad (1.27)$$

$$A_W^H(\tau) = -[2 + 3\tau + 3\tau(2 - \tau)f(\tau)], \quad (1.28)$$

with the function $f(\tau)$ defined in Eq. (1.24). The parameters $\tau_i = 4M_i^2/M_H^2$ ($i = f, W$) are defined by the corresponding masses of the heavy loop particles. N_{cf} denotes again the colour factor of the fermion and e_f its electric charge. For large loop masses the form factors approach constant values,

$$\begin{aligned} A_f^H &\rightarrow \frac{4}{3} && \text{for } M_H^2 \ll 4M_Q^2 \\ A_W^H &\rightarrow -7 && \text{for } M_H^2 \ll 4M_W^2. \end{aligned} \quad (1.29)$$

The W loop provides the dominant contribution in the intermediate Higgs mass regime, and the fermion loops interfere destructively. The QCD corrections have been calculated and are small in the intermediate Higgs boson mass region. [Zheng, Wu; Djouadi, Graudenz Spira, Zerwas; Melnikov, Spira, Yakovlev; Dawson, Kauffmann; Melnikov, Yakovlev; Inoue, Najima, Okada, Saito] The tree-level decay width into $Z\gamma$ is given

$$\Gamma(H \rightarrow Z\gamma) = \frac{G_F^2 M_W^2 \alpha M_H^3}{64\pi^4} \left(1 - \frac{M_Z^2}{M_H^2}\right)^3 \left| \sum_f A_f^H(\tau_f, \lambda_f) + A_W^H(\tau_W, \lambda_W) \right|^2, \quad (1.30)$$

with the form factors

$$\begin{aligned} A_f^H(\tau, \lambda) &= 2N_{cf} \frac{e_f(I_{3f} - 2e_f \sin^2 \theta_W)}{\cos \theta_W} [I_1(\tau, \lambda) - I_2(\tau, \lambda)] \\ A_W^H(\tau, \lambda) &= \cos \theta_W \left\{ 4(3 - \tan^2 \theta_W) I_2(\tau, \lambda) \right. \\ &\quad \left. + \left[\left(1 + \frac{2}{\tau}\right) \tan^2 \theta_W - \left(5 + \frac{2}{\tau}\right) \right] I_1(\tau, \lambda) \right\}. \end{aligned} \quad (1.31)$$

The functions I_1 and I_2 read

$$I_1(\tau, \lambda) = \frac{\tau\lambda}{2(\tau - \lambda)} + \frac{\tau^2\lambda^2}{2(\tau - \lambda)^2} [f(\tau) - f(\lambda)] + \frac{\tau^2\lambda}{(\tau - \lambda)^2} [g(\tau) - g(\lambda)] \quad (1.32)$$

$$I_2(\tau, \lambda) = -\frac{\tau\lambda}{2(\tau - \lambda)} [f(\tau) - f(\lambda)]. \quad (1.33)$$

The function $g(\tau)$ can be cast into the form

$$g(\tau) = \begin{cases} \sqrt{\tau - 1} \arcsin \frac{1}{\sqrt{\tau}} & \tau \geq 1 \\ \frac{\sqrt{1 - \tau}}{2} \left[\log \frac{1 + \sqrt{1 - \tau}}{1 - \sqrt{1 - \tau}} - i\pi \right] & \tau < 1 \end{cases} \quad (1.34)$$

The parameters $\tau_i = 4M_i^2/M_H^2$ and $\lambda_i = 4M_i^2/M_Z^2$ ($i = f, W$) are defined in terms of the corresponding masses of the heavy loop particles. The W loop dominates in the intermediate Higgs mass range, and the heavy fermion loops interfere destructively.

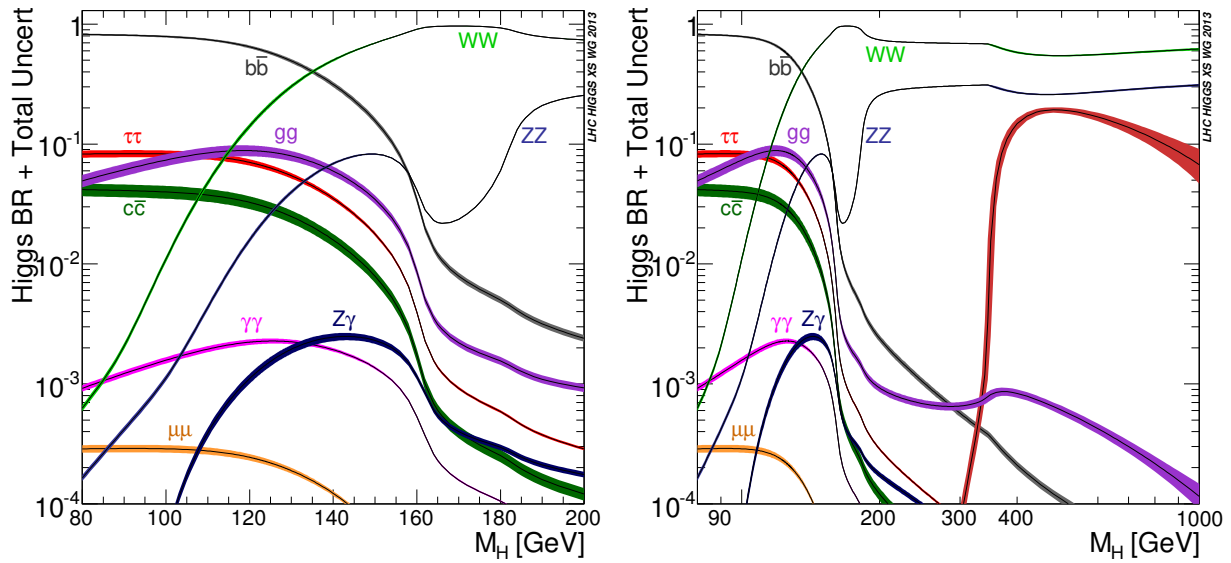


Figure 1.2: The Higgs boson branching ratios as a function of the Higgs boson mass: zoomed in low-mass region (left), whole canonical mass region (right). Plot taken from the LHC Higgs Cross Section Working Group Report 3 [8].

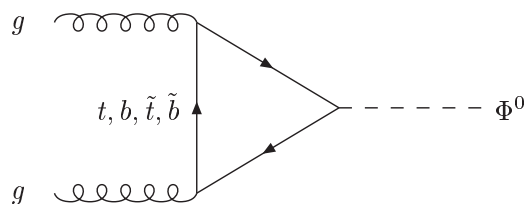
Figs. 1.2 and 1.3 show plots as they were already produced before the Higgs boson discovery when the Higgs boson mass was still unknown. Shown are the Higgs boson branching ratios and total width, respectively, as a function of the Higgs boson mass. One can infer from the figures that the total Higgs boson width is rather small, less than ~ 10 MeV, for masses below about 140 GeV. Once the threshold for gauge boson decays is reached the total width increases rapidly up to about 600 GeV for $M_H = 1$ TeV. The gauge boson decay widths are proportional to M_H^3 . Below the gauge boson threshold the main decay is into $b\bar{b}$, followed by the decay into $\tau^+\tau^-$. - The error bands include the parametric and theoretical uncertainties.

1.5 Higgs boson production at the LHC

There are several Higgs boson production mechanisms at the LHC.

- Gluon fusion: The dominant production mechanism for Standard Model Higgs bosons at the LHC is gluon fusion

[Georgi, et al.;Gamberini, et al.]



$$pp \rightarrow gg \rightarrow H .$$

$$(1.35)$$

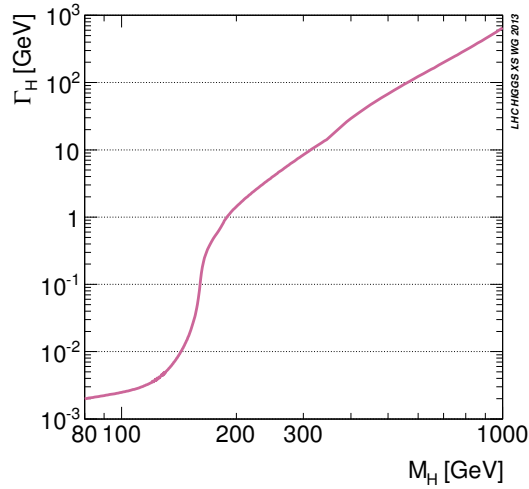


Figure 1.3: The Higgs boson total width as a function of the Higgs boson mass. Plot taken from the LHC Higgs Cross Section Working Group Report 3 [8].

In the Standard Model it is mediated by top and bottom quark loops. The QCD corrections (the next-to leading order calculation involves 2-loop diagrams!) have been calculated and turn out to be large. They are of the order 10-100%. [Spira, Djouadi, Graudenz, Zerwas; Dawson, Kauffmann, Schaffer]; see Fig. 1.4, which shows the NLO K -factor, *i.e.* the ratio of the NLO cross section to the leading order (LO) cross section as a function of the Higgs boson mass for the virtual and real corrections.

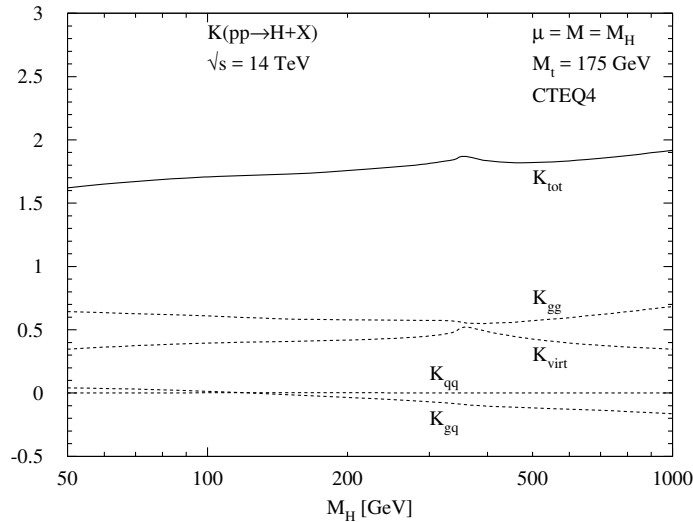


Figure 1.4: The K factor for the gluon fusion process as a function of the Higgs boson mass.

Due to the inclusion of the NLO QCD corrections the scale dependence of the gluon fusion cross section is decreased, *cf.* Fig. 1.5.

The next-to-next-to leading order (NNLO) corrections have been calculated in the limit of heavy top quark masses ($M_H \ll m_t$) [Harlander,Kilgore;Anastasiou,Melnikov;Ravindran,...].

They lead to a further increase of the cross section by 20-30%. The scale dependence is reduced to $\Delta \lesssim 10 - 15\%$. Resummation of the soft gluons [Catani, et al.; ...] adds another 10%. There has been a lot of progress in the computation of the higher-order corrections to

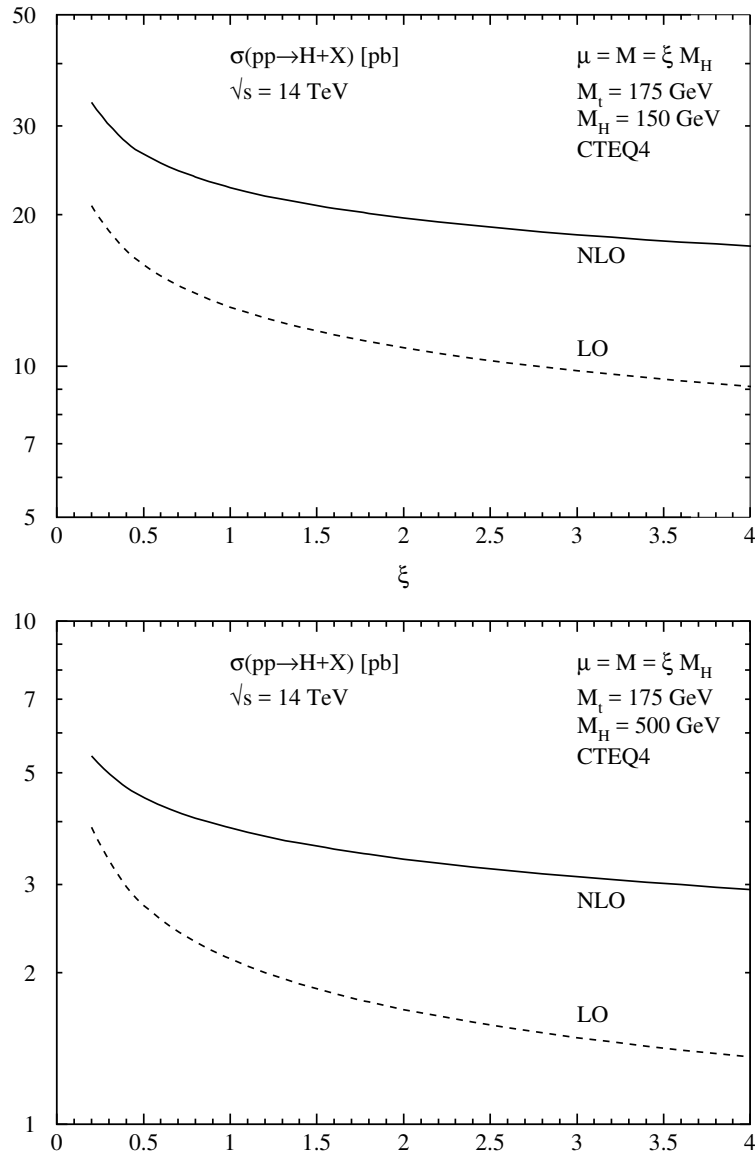


Figure 1.5: The scale dependence of the gluon fusion cross section for two different Higgs boson masses.

gluon fusion in the last years.
Status of higher order (HO) corrections:

- ▷ complete NLO: increase σ by $\sim 10-100\%$
- ▷ SM: limit $M_\Phi \ll m_t$ - approximation $\sim 20-30\%$
- ▷ NNLO @ $M_\Phi \ll m_t \Rightarrow$ further increase by 20-30%

top mass effects are small in the SM

- ▷ NNNLO for $M_\Phi \ll m_t \rightsquigarrow$ scale stabilisation

scale dependence: $\Delta \lesssim 5\%$

- ▷ NNNLL soft resummation: $\sim 2\%$
- ▷ leading soft contribution at N³LO in limit $m_t \rightarrow \infty$
- ▷ SM+2HDM EW corrections $\sim 5\%$
- ▷ impl. in POWHEG including mass effects at NLO

Spira,Djouadi,Graudenz,Zerwas
Dawson;Kauffman,Schaffer

Krämer,Laenen,Spira

Harlander,Kilgore

Anastasiou,Melnikov

Ravindran,Smith,van Neerven

Marzani,Ball,Del Duca,Forte,Vicini

Harlander,Ozeren

Pak,Rogal,Steinhauser

Moch,Vogt

Ravindran

de Florian,Mazzitelli,Moch,Vogt

Anastasiou,Duhr,Dulat,Furlan,Gehrmann,Herzog,Mistlberger

Ball,Bonvini,Forte,Marzani,Ridolfi

Catani,de Florian,Grazzini,Nason

Ravindran

Ahrens,Becher,Neubert,Yang

Ball,Bonvini,Forte,Marzani,Ridolfi

Bonvini,Marzani

Schmidt,Spira

Ravindran,Smith,van Neerven; Ahrens eal

Aglietti eal

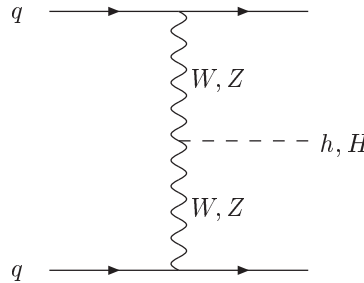
Degrassi,Maltoni

Actis,Passarino,Sturm,Uccirati

Jennis,Sturm,Uccirati

Bagnaschi,Degrassi,Slavich,Vicini

- WW/ZZ fusion: Higgs bosons can be produced in the WW/ZZ fusion processes [Cahn, Dawson; Hikasa; Altarelli, Mele, Pitolli]

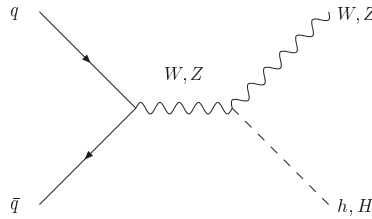


$$pp \rightarrow W^*W^*/Z^*Z^* \rightarrow H . \quad (1.36)$$

The QCD corrections have been calculated long time ago and amount up to $\sim 10\%$ [Han, Valencia, Willenbrock], [Figy,Oleary,Zeppenfeld], [Berger,Campbell]. In the meantime more higher-order QCD and EW corrections have been calculated.

- ▷ approximate 2-loop QCD corrs. $\Rightarrow \lesssim 1\%$ Bolzano,Maltoni,Moch,Zaro
Cacciari,Dreyer,Karlberg,Salam,Zanderighi
- ▷ approximate 3-loop QCD corrs. $\Rightarrow \lesssim 0.3\%$ Dreyer,Karlberg
- ▷ electroweak corrs. $\Rightarrow \sim 10\%$ Ciccolini,Denner,Dittmaier

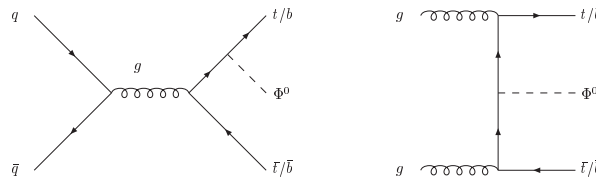
- Higgs-strahlung: Higgs boson production in Higgs-strahlung [Glashow et al.; Kunszt et al.] proceeds via



$$pp \rightarrow W^*/Z^* \rightarrow W/Z + H . \quad (1.37)$$

The QCD corrections are $\sim 30\%$ [Han,Willenbrock]. The NNLO QCD corrections add another $\lesssim 5\%$ [Harlander, Kilgore; Hamberg, Van Neerven, Matsuura; Brein, Djouadi, Harlander]. The theoretical error is reduced to about 5%. The complete electroweak (EW) corrections reduce the cross section by 5-10% [Ciccolini, Dittmaier, Krämer]. Furthermore, the $W/Z + H$ production has been provided fully exclusively at NNLO QCD [Ferrera,Grazzini,Tramantano].

- Associated Production: Higgs bosons can also be produced in association with top and bottom quarks [Kunszt; Gunion; Marcano, Paige]



$$pp \rightarrow t\bar{t}/b\bar{b} + H . \quad (1.38)$$

The process $t\bar{t}H \rightarrow t\bar{t}b\bar{b}$ is important at the LHC as it gives access to the top Yukawa coupling. The NLO QCD corrections to associated top production increase the cross section at the LHC by 20% [Beenakker, et al.; Dawson, et al.]. The parton level cross section has been linked to parton showers in the tools `aMC@NLO` and `PowHel` [Frederix et al.; Garzelli,Kardos,Papadopoulos,Trocsanyi]. There has been important work on the background $t\bar{t}b\bar{b}$, $t\bar{t}jj$ etc. [Bredenstein,Denner,Dittmaier,Pozzorini; Bevilacqua,Czakon,Papadopoulos,Pittau,Worek; Cascioli,Maierhofer,Pozzorini] Fig. 1.5 shows the production cross sections in pb as a function of the Higgs boson mass. The bands show the residual theoretical error.

1.6 Higgs Boson Discovery

The main Higgs discovery channels are the $\gamma\gamma$ and Z^*Z^* final states. The decay into $\gamma\gamma$ final states has a very small branching ratio, but is very clean. (CMS and ATLAS have an excellent photon-energy resolution. Look for narrow $\gamma\gamma$ invariant mass peak, extrapolate background into the signal region from thresholds.). The Z^*Z^* final state is the other important search channel. For $M_H = 125$ GeV it is an off-shell decay. It leads to a clean 4 lepton (4l) final state from the decay of the Z bosons. Also the WW final state is off-shell. The final state signature includes missing energy from the neutrinos of the W boson decays. The $b\bar{b}$ final state is exploited as well. It has the largest branching ratio, but suffers from a large QCD

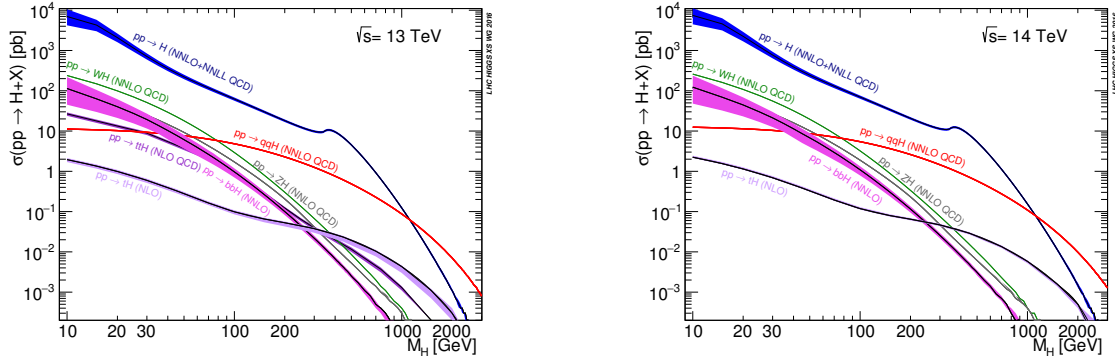


Figure 1.6: The Higgs boson production cross sections at the LHC as a function of the Higgs boson mass for a center-of-mass energy of 13 TeV (left) and 14 TeV (right).

background. Finally, the $\tau\tau$ channel is also used.

The main discovery channels for the 125 GeV Higgs boson at ATLAS and CMS, *i.e.* the photon and the Z boson final states, are shown in Fig. 1.7.

The experiments give the best fit values to the reduced μ values in the final state X . These are the production rate times branching ratio into the final state $X = \gamma, Z, W, b, \tau$ normalized to the corresponding value for a SM Higgs boson,

$$\mu = \frac{\sigma_{\text{prod}} \times BR(H \rightarrow XX)}{(\sigma_{\text{prod}} \times BR(H \rightarrow XX))_{\text{SM}}} . \quad (1.39)$$

In case the discovered Higgs boson is a SM Higgs boson they are all equal to 1. Figure 1.8 shows the μ values reported by the LHC experiments. The various final states suffer from uncertainties that leave room for beyond the SM (BSM) physics.

1.7 Higgs boson couplings at the LHC

In principle the strategy to measure the Higgs boson couplings is to combine various Higgs production and decay channels, from which the couplings can then be extracted. For example, the production of the Higgs boson in W boson fusion with subsequent decay into τ leptons, Fig. 1.9, is proportional to the partial width into WW and the branching ratio into $\tau\tau$. Combination with other production/decay channels and the knowledge of the total width allow then to extract the Higgs couplings. The problem at the LHC, however, is that the total width, which is small for a SM 125 GeV Higgs boson, cannot be measured without model-assumptions, and also not all final states are accessible experimentally. Therefore without applying model-assumptions only ratios of couplings are measurable.

The theoretical approach is to define an effective Lagrangian with modified Higgs couplings. In a first approach the couplings are modified by overall scale factors κ_i and the tensor structure is not changed. With this Lagrangian the signal rates, respectively μ values, are calculated as function of the scaling factors, $\mu(\kappa_i)$. These are then fitted to the experimentally measured μ values. The fits provide then the κ_i values. Such a theoretical

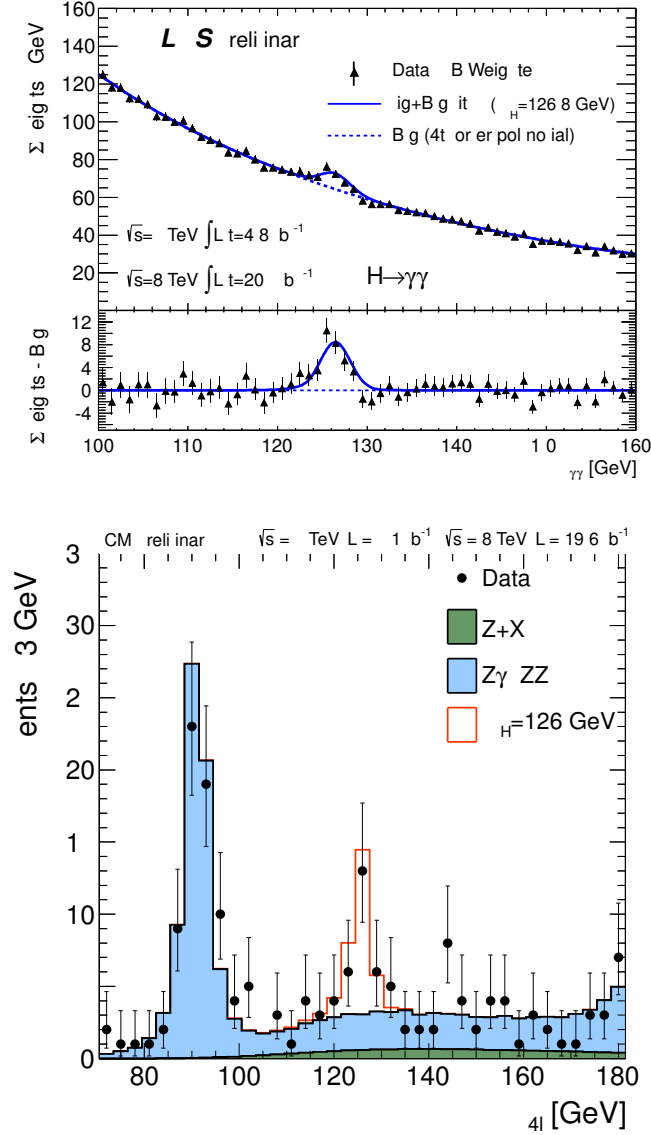


Figure 1.7: The main Higgs discovery channels: Upper: The photon final state, here shown for the ATLAS experiment [ATLAS-CONF-2013-12]. Lower: The Z^*Z^* final state, here shown for the CMS experiment [CMS-PAS-HIG-13-002].

Lagrangian for the SM field content with a scalar particle h looks like

$$\begin{aligned} \mathcal{L} = & \mathcal{L}_h - (M_W^2 W_\mu^+ W^{\mu-} + \frac{1}{2} M_Z^2 Z_\mu Z^\mu) [1 + 2\kappa_V \frac{h}{v} + \mathcal{O}(h^2)] \\ & - m_{\psi_i} \bar{\psi}_i \psi_i [1 + \kappa_F \frac{h}{v} + \mathcal{O}(h^2)] + \dots \end{aligned} \quad (1.40)$$

It is valid below the scale Λ where new physics (NP) becomes important. It implements the electroweak symmetry breaking (EWSB) via \mathcal{L}_h and the custodial symmetry through $\kappa_W = \kappa_Z = \kappa_V$. Furthermore, there are no tree-level flavour changing neutral current (FCNC) couplings as κ_F is chosen to be the same for all fermion generations and does not allow for transitions between fermion generations. The best fit values for κ_f and κ_V are

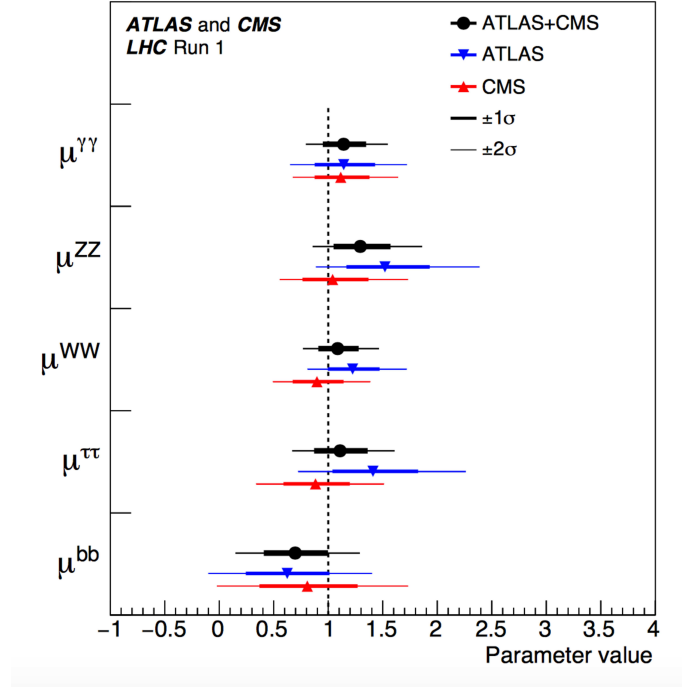


Figure 1.8: Combined best fits for the μ values from the ATLAS and CMS experiments based on Run 1 data.

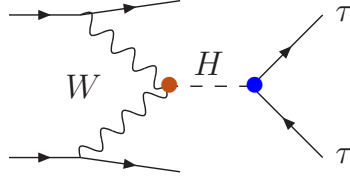


Figure 1.9: Feynman diagram for the production of a Higgs boson in W boson fusion with subsequent decay into $\tau\tau$. It is proportional to the partial width Γ_{WW} and the branching ratio into $\tau\tau$, $\text{BR}(H \rightarrow \tau\tau)$.

shown in Fig. 1.10.

If the discovered particle is the Higgs boson the coupling strengths are proportional to the masses (squared) of the particles to which the Higgs boson couples. This trend can be seen in the plot published by CMS, see Fig. 1.11.

1.8 Higgs Boson Quantum Numbers

The Higgs boson quantum numbers can be extracted by looking at the threshold distributions and the angular distributions of various production and decay processes. The SM Higgs

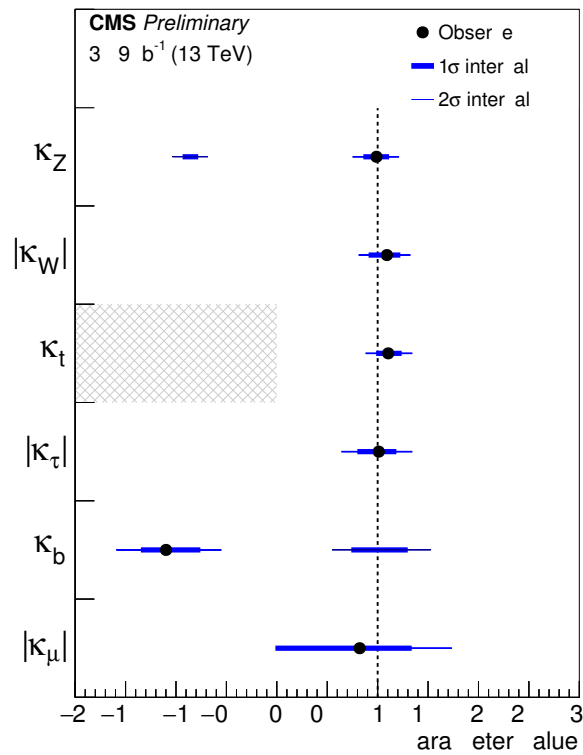
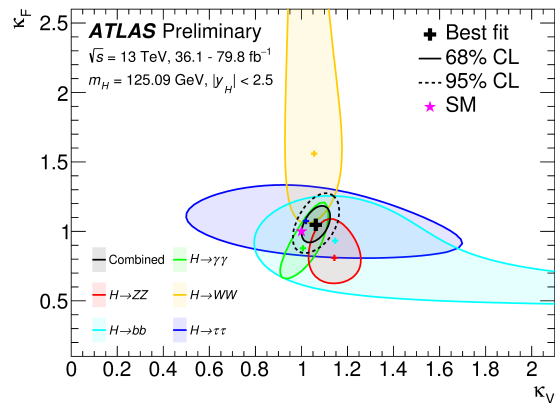


Figure 1.10: The best fit values for κ_f and κ_V by ATLAS (upper). The best fit values to the κ 's measured by CMS [CMS-PAS-HIG-17-031] (lower).

boson has spin 0, positive parity P and is even under charge conjugation C . From the observation of the Higgs boson in the $\gamma\gamma$ final state one can already conclude that it does not have spin 1, due to the Landau-Yang theorem, and that it has $C = +1$, assuming charge invariance. However, these are theoretical considerations and have to be proven also experimentally.

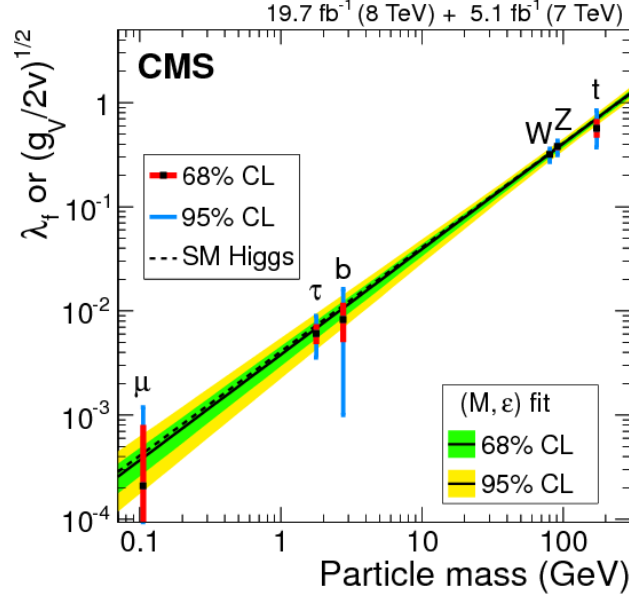


Figure 1.11: Coupling strengths as function of the mass of the particles coupled to the Higgs boson.

The theoretical tools to provide angular distributions for a particle with arbitrary spin and parity are helicity analyses and operator expansion. Let us look as an example at the Higgs decay into ZZ^* , and the Z bosons subsequently decay into 4 leptons,

$$H \rightarrow ZZ^{(*)} \rightarrow (f_1\bar{f}_1)(f_2\bar{f}_2). \quad (1.41)$$

The decay is illustrated in Fig. 1.12. The angle φ is the azimuthal angle between the decay planes of the Z bosons in the H rest frame. The θ_1 and θ_2 are the polar angles, respectively, of the fermion pairs in, respectively, the rest frame of the decaying Z boson.

For the SM the double polar angle distribution reads

$$\frac{1}{\Gamma'} \frac{d\Gamma'}{d\cos\theta_1 d\cos\theta_2} = \frac{9}{16} \frac{1}{\gamma^4 + 2} \left[\gamma^4 \sin^2\theta_1 \sin^2\theta_2 + \frac{1}{2} (1 + \cos^2\theta_1)(1 + \cos^2\theta_2) \right] \quad (1.42)$$

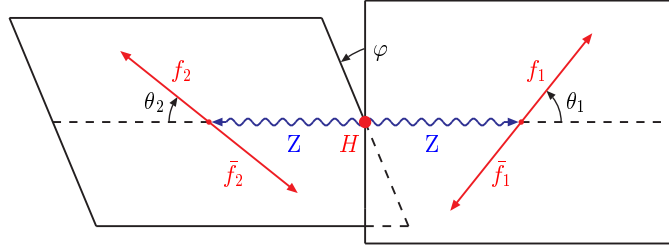
and the azimuthal angular distribution is given by

$$\frac{1}{\Gamma'} \frac{d\Gamma'}{d\phi} = \frac{1}{2\pi} \left[1 + \frac{1}{2} \frac{1}{\gamma^4 + 2} \cos 2\phi \right] \quad (1.43)$$

The verification of these distributions is a necessary step for the proof of the 0^+ nature of the Higgs boson.

The calculation of the azimuthal angular distribution delivers a different behaviour for a scalar and a pseudoscalar boson:

$$\begin{aligned} 0^+ &: d\Gamma/d\phi \sim 1 + 1/(2\gamma^4 + 4) \cos 2\phi \\ 0^- &: d\Gamma/d\phi \sim 1 - 1/4 \cos 2\phi \end{aligned} \quad (1.44)$$

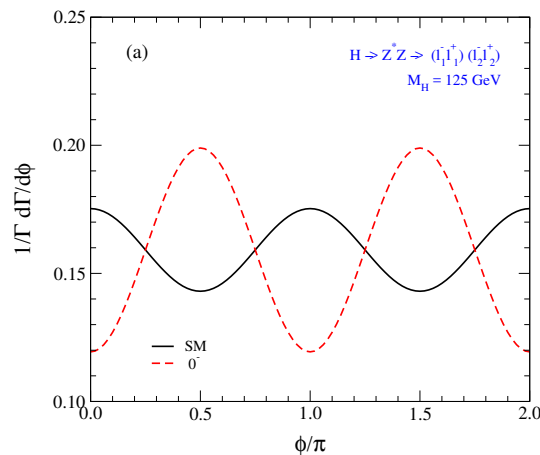

 Figure 1.12: The decay $H \rightarrow ZZ^* \rightarrow (f_1 \bar{f}_1)(f_2 \bar{f}_2)$.

Here $\gamma^2 = (M_H^2 - M_*^2 - M_Z^2)/(2M_*M_Z)$ and M_* is the mass of the virtual Z boson. Figure 1.13 shows how the azimuthal angular distribution can be exploited to test the parity of the particle. A pseudoscalar with spin-parity 0^- shows the opposite behaviour in this distribution than the scalar, which is due to the minus sign in front of $\cos 2\phi$ in Eq. (1.44). The threshold behaviour on the other hand can be used to determine the spin of the particle. We have for spin 0 a linear rise with the velocity β ,

$$\frac{d\Gamma[H \rightarrow Z^*Z]}{dM_*^2} \sim \beta = \sqrt{(M_H - M_Z)^2 - M_*^2}/M_H. \quad (1.45)$$

A spin 2 particle, *e.g.* shows a flatter rise, $\sim \beta^3$, *cf.* Fig. 1.14.

The experiments cannot perform an independent spin-parity measurement. Instead they test various spin-parity hypotheses. Various non-SM spin-parity hypotheses have been ruled out at more than 95% confidence level (C.L.), see *e.g.* Fig. 1.15.


 Figure 1.13: The azimuthal distribution for the $H \rightarrow ZZ^* \rightarrow 4l$ decay for the SM scalar Higgs (black) and a pseudoscalar (red). [Choi,Mühlleitner,Zerwas]

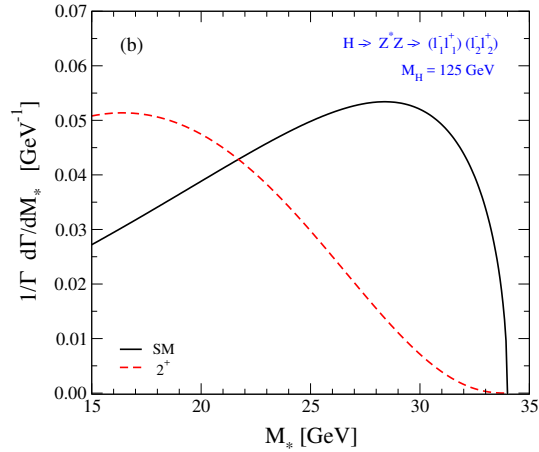


Figure 1.14: The threshold distribution for the $H \rightarrow ZZ^* \rightarrow 4l$ decay for the SM spin-0 Higgs (black) and a spin-2 particle (red).[Choi,Mühlleitner,Zerwas]

1.9 Determination of the Higgs self-interactions

In order to fully establish the Higgs mechanism as the one responsible for the generation of particle masses without violating gauge principles, the Higgs potential has to be reconstructed. This can be done once the Higgs trilinear and quartic self-interactions have been measured. The trilinear coupling λ_{HHH} is accessible in double Higgs production. The quartic coupling λ_{HHHH} is to be obtained from triple Higgs production.

1.9.1 Determination of the Higgs self-couplings at the LHC

The processes for the extraction of λ_{HHH} [Djouadi,Kilian,Mühlleitner,Zerwas] at the LHC are gluon fusion into a Higgs pair, double Higgs-strahlung, WW/ZZ fusion and radiation of a Higgs pair off top quarks.

$$\begin{array}{llll}
 \text{gluon fusion:} & gg & \rightarrow & HH \\
 \text{double Higgs-strahlung:} & q\bar{q} & \rightarrow & W^*/Z^* \rightarrow W/Z + HH \\
 \text{WW/ZZ double Higgs fusion:} & qq & \rightarrow & qq + WW/ZZ \rightarrow HH \\
 \text{associated production:} & pp & \rightarrow & t\bar{t}HH
 \end{array} \tag{1.46}$$

The dominant gluon fusion production process proceeds via triangle and box diagrams, see Fig. 1.16.

Due to smallness of the cross sections, *cf.* Fig. 1.17, and the large QCD background the extraction of the Higgs self-coupling at the LHC is extremely difficult. There is an enormous theoretical activity to determine the production processes with high accuracy including HO corrections and to develop strategies and observables for the measurement of the di-Higgs production processes and the trilinear Higgs self-couplings. Status of higher order (HO) corrections:

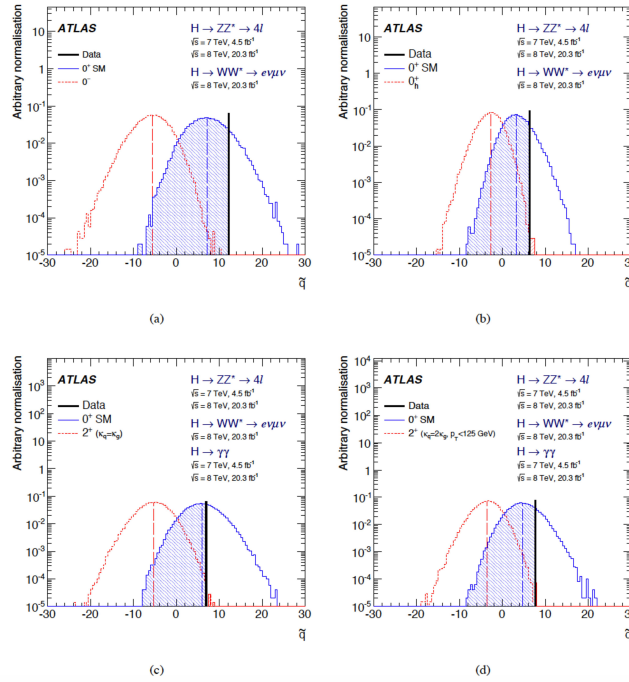


Figure 1.15: Examples of distributions of the test statistic \tilde{q} for the combination of decay channels. (a): 0^+ versus 0 ; (b): 0^+ versus 0_h^+ ; (c): 0^+ versus the spin-2 model with universal couplings ($\kappa_q = \kappa_g$); (d): 0^+ versus the spin-2 model with $\kappa_q = 2\kappa_g$ and the p_T selection at 125 GeV. The observed values are indicated by the vertical solid line and the expected medians by the dashed lines. The shaded areas correspond to the integrals of the expected distributions used to compute the p -values for the rejection of each hypothesis. Figure taken from and details in Eur. Phys. J. C75 (2015) no.10, 476, Erratum: Eur. Phys. J. C76 (2016) no.3, 152.

- ▷ LO cxn known exactly with full mass dependence
 - ▷ NLO QCD corrections - multi-scale problem
 - ▷ improved LET: $K = \sigma_{\text{NLO}}/\sigma_{\text{LO}} \sim 1.7$
 - ▷ Estimate of finite mass effects: inclusion of higher-order corr. in large m_t exp. $\mathcal{O}(\pm 10\%)$
 - ▷ real contribution w/ full m_t dependence \rightsquigarrow top mass effects: $\mathcal{O}(-10\%)$
 - ▷ Full NLO calculation \rightsquigarrow top mass effects: -14%
 - ▷ NNLO QCD corr. for expansion in small external momenta: $\mathcal{O}(20\%)$
 - ▷ threshold resumm., further increase NNLO+NNLL in large top mass limit NLL w/ top quark mass effects
 - ▷ Theoretical uncertainty: scale 6%, pdf 2%, α_s 2%
- Glover, van der Bij '88;
 Plehn, Spira, Zerwas '95

 Dawson, Dittmaier, Spira '98
 Grigo, Hoff, Melnikov, Steinhauser '13;
 Grigo, Hoff, Steinhauser '15;
 Degrossi, Giardino, Gröber '16

 Frederix, Frixione, Hirschi,
 Maltoni, Mattelaer, Torrielli,
 Vryonidou, Zaro '14

 Borowka et al '16
 de Florian, Mazzitelli '13 '15;
 Grigo, Melnikov, Steinhauser '14;
 Grigo, Hoff, Steinhauser '15;
 de Florian, Grazzini, Hanga, Kallweit,
 Lindert, Maierhöfer, Mazzitelli, Rathlev '16

 de Florian, Mazzitelli '15
 Ferrara, Pires '16

 LHC Higgs Cross Section WG

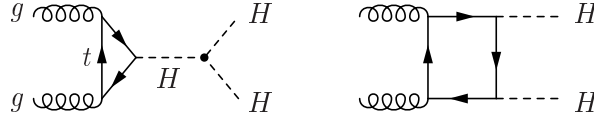


Figure 1.16: The diagrams that contribute to the gluon fusion process $gg \rightarrow HH$.

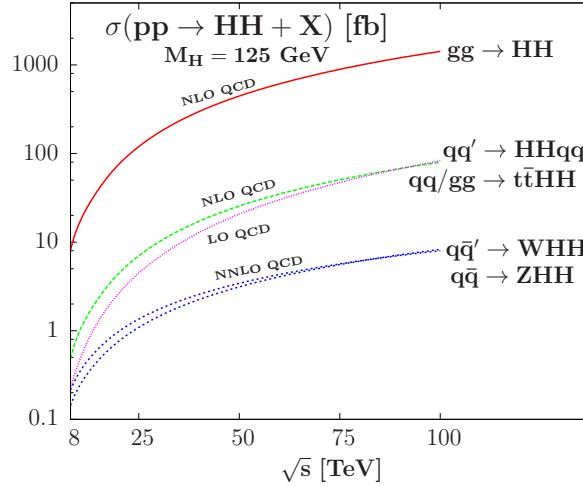


Figure 1.17: Di-Higgs production processes at the LHC with c.m. energy 14 TeV, including higher-order corrections. [Baglio,Djouadi,Gröber,Mühlleitner,Quévillon,Spira].

The next-to-leading order cross section for Higgs pair production at a c.m. energy of 14 TeV amounts to [Borowka eal '16]

$$\sigma_{gg \rightarrow HH}^{\text{NLO}} = 32.91_{-12.6\%}^{+13.6\%} \text{ fb} . \quad (1.47)$$

The current constraints on the SM trilinear Higgs self-coupling are [arXiv:1506.0028, 1509.0467, 1603.0689; ATLAS-CONF-2016-049] $\mathcal{O}(\pm 15 \lambda_{hhh}^{\text{SM}})$, *cf.* Fig. 1.18. The prospects in the $b\bar{b}\gamma\gamma$ final state are [ATL-PHYS-PUB-2017-001] $-0.8 < \lambda_{hh}/\lambda_{hhh}^{\text{SM}} < 7.7$.

1.10 Summary

The measurements of the properties of the discovered particle have identified it as the Higgs boson. CERN therefore officially announced in a press release of March 2013 that the discovered particle is the Higgs boson, *cf.* Fig. 1.19. This lead then to the Nobel Prize for Physics in 2013 to Francois Englert and Peter Higgs.

The SM of particle physics has been very successful so far. At the experiments it has been tested to highest accuracy, including higher order corrections. And with the discovery of the Higgs particle we have found the last missing piece of the SM of particle physics. Still there are many open questions that cannot be answered by the SM. To name a few of them

1. In the SM the Higgs mechanism is introduced ad hoc. There is no dynamical mechanism behind it.

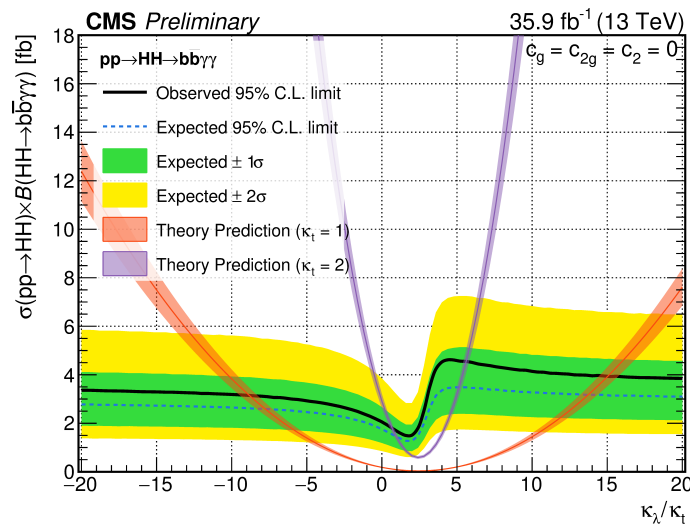


Figure 1.18: Plot taken from CMS-PAS-HIG-17-008.

2. In the presence of high energy scales, the Higgs boson mass receives large quantum corrections, inducing the hierarchy problem.
3. We have no explanation for the fermion masses and mixings.
4. The SM does not contain a Dark Matter candidate.
5. In the SM the gauge couplings do not unify.
6. The SM does not incorporate gravity.
7. The CP violation in the SM is not large enough to allow for baryogenesis.
8. ...

We therefore should rather see the SM as an effective low-energy theory which is embedded in some more fundamental theory that becomes apparent at higher scales. The Higgs data so far, although pointing towards a SM Higgs boson, still allow for interpretations within theories beyond the SM. These BSM theories can solve some of the problems of the SM. A few of these BSM models shall be presented in this lecture.

CERN press office

[Media visits](#) [Press releases](#) [For journalists](#) [For CERN people](#) [Contact us](#)

New results indicate that particle discovered at CERN is a Higgs boson

14 Mar 2013

Geneva, 14 March 2013. At the Moriond Conference today, the ATLAS and CMS collaborations at CERN¹'s Large Hadron Collider (LHC) presented preliminary new results that further elucidate the particle discovered last year. Having analysed two and a half times more data than was available for the discovery announcement in July, they find that the new particle is looking more and more like a Higgs boson, the particle linked to the mechanism that gives mass to elementary particles. It remains an open question, however, whether this is the Higgs boson of the Standard Model of particle physics, or possibly the lightest of several bosons predicted in some theories that go beyond the Standard Model. Finding the answer to this question will take time.

Figure 1.19: CERN press release.

Chapter 2

Appendix

2.1 Beispiel: Feldtheorie für ein komplexes Feld

Wir betrachten die Lagrangedichte für ein komplexes Skalarfeld

$$\mathcal{L} = (\partial_\mu \phi)^* (\partial^\mu \phi) - \mu^2 \phi^* \phi - \lambda (\phi^* \phi)^2 \quad \text{mit dem Potential} \quad V = \mu^2 \phi^* \phi + \lambda (\phi^* \phi)^2. \quad (2.1)$$

(Hinzufügen höherer Potenzen in ϕ führt zu einer nicht-renormierbaren Theorie.) Die Lagrangedichte ist invariant unter einer $U(1)$ -Symmetrie,

$$\phi \rightarrow \exp(i\alpha) \phi. \quad (2.2)$$

Wir betrachten den Grundzustand. Dieser ist gegeben durch das Minimum von V ,

$$0 = \frac{\partial V}{\partial \phi^*} = \mu^2 \phi + 2\lambda (\phi^* \phi) \phi \quad \Rightarrow \quad \phi = \begin{cases} 0 & \text{für } \mu^2 > 0 \\ \phi^* \phi = -\frac{\mu^2}{2\lambda} & \text{für } \mu^2 < 0 \end{cases} \quad (2.3)$$

Der Parameter λ muß positiv sein, damit das System nicht instabil wird. Für $\mu^2 < 0$ nimmt das Potential die Form eines Mexikanerhutes an, siehe Fig. 2.1. Bei $\phi = 0$ liegt ein lokales Maximum, bei

$$|\phi| = v = \sqrt{-\frac{\mu^2}{2\lambda}} \quad (2.4)$$

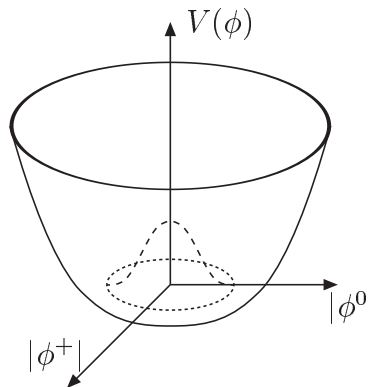


Figure 2.1: Das Higgspotential.

ein globales Minimum. Teilchen entsprechen harmonischen Oszillatoren für die Entwicklung um das Minimum des Potentials. Fluktuationen in Richtung der (unendlich vielen degenerierten) Minima besitzen Steigung null und entsprechen masselosen Teilchen, den Goldstone Bosonen. Fluktuationen senkrecht zu dieser Richtung entsprechen Teilchen mit Masse $m > 0$. Die Entwicklung um das Maximum bei $\phi = 0$ würde zu Teilchen negativer Masse (Tachyonen) führen, da die Krümmung des Potentials hier negativ ist.

Entwicklung um das Minimum bei $\phi = v$ führt zu (wir haben für das komplexe skalare Feld zwei Fluktuationen φ_1 und φ_2)

$$\phi = v + \frac{1}{\sqrt{2}}(\varphi_1 + i\varphi_2) = \left(v + \frac{1}{\sqrt{2}}\varphi_1 \right) + i\frac{\varphi_2}{\sqrt{2}} \quad \Rightarrow \quad (2.5)$$

$$\phi^*\phi = v^2 + \sqrt{2}v\varphi_1 + \frac{1}{2}(\varphi_1^2 + \varphi_2^2). \quad (2.6)$$

Damit erhalten wir für das Potential

$$V = \lambda(\phi^*\phi - v^2)^2 - \frac{\mu^4}{4\lambda^2} \quad \text{mit} \quad v^2 = -\frac{\mu^2}{2\lambda} \quad \Rightarrow \quad (2.7)$$

$$V = \lambda \left(\sqrt{2}v\varphi_1 + \frac{1}{2}(\varphi_1^2 + \varphi_2^2) \right)^2 - \frac{\mu^4}{4\lambda^2}. \quad (2.8)$$

Vernachlässige den letzten Term in V , da es sich nur um eine konstante Nullpunktsverschiebung handelt. Damit ergibt sich für die Lagrangedichte

$$\mathcal{L} = \frac{1}{2}(\partial_\mu\varphi_1)^2 + \frac{1}{2}(\partial_\mu\varphi_2)^2 - 2\lambda v^2\varphi_1^2 - \sqrt{2}v\lambda\varphi_1(\varphi_1^2 + \varphi_2^2) - \frac{\lambda}{4}(\varphi_1^2 + \varphi_2^2)^2. \quad (2.9)$$

Die in den Feldern quadratischen Terme liefern die Massen, die in den Feldern kubischen und quartischen Terme sind die Wechselwirkungsterme. Es gibt ein massives und ein masseloses Teilchen,

$$m_{\varphi_1} = 2v\sqrt{\lambda} \quad \text{und} \quad m_{\varphi_2} = 0. \quad (2.10)$$

Bei dem masselosen Teilchen handelt es sich um das Goldstone Boson.

Bibliography

- [1] J. Goldstone, A. Salam and S. Weinberg, Phys. Rev. **127** (1962) 965; S. Weinberg, Phys. Rev. Lett. **19** (1967) 1264; S.L. Glashow, S. Weinberg, Phys. Rev. Lett. **20** (1968) 224; A. Salam, Proceedings Of The Nobel Symposium, Stockholm 1968, ed. N. Svartholm.
- [2] P.W. Higgs, Phys. Lett. **12** (1964) 132; Phys. Rev. Lett. **13** (1964) 508 and Phys. Rev. **145** (1966) 1156; F. Englert and R. Brout, Phys. Rev. Lett. **13** (1964) 321; G.S. Guralnik, C.R. Hagen and T.W. Kibble, Phys. Rev. Lett. **13** (1964) 585.
- [3] G. Aad *et al.* [ATLAS Collaboration], Phys. Lett. B **716** (2012) 1 doi:10.1016/j.physletb.2012.08.020 [arXiv:1207.7214 [hep-ex]].
- [4] S. Chatrchyan *et al.* [CMS Collaboration], Phys. Lett. B **716** (2012) 30 doi:10.1016/j.physletb.2012.08.021 [arXiv:1207.7235 [hep-ex]].
- [5] A. Djouadi, J. Kalinowski and M. Spira, Comput. Phys. Commun. **108** (1998) 56 doi:10.1016/S0010-4655(97)00123-9 [hep-ph/9704448].
- [6] A. Djouadi, J. Kalinowski, M. Muehlleitner and M. Spira, arXiv:1801.09506 [hep-ph].
- [7] S. Dittmaier *et al.*, doi:10.5170/CERN-2012-002 arXiv:1201.3084 [hep-ph].
- [8] S. Heinemeyer *et al.* [LHC Higgs Cross Section Working Group], doi:10.5170/CERN-2013-004 arXiv:1307.1347 [hep-ph].
- [9] D. de Florian *et al.* [LHC Higgs Cross Section Working Group], doi:10.23731/CYRM-2017-002 arXiv:1610.07922 [hep-ph].
- [10] S. Kanemura, Y. Okada, E. Senaha and C.-P. Yuan, Phys. Rev. D **70** (2004) 115002 [hep-ph/0408364].
- [11] G. C. Branco, P. M. Ferreira, L. Lavoura, M. N. Rebelo, M. Sher and J. P. Silva, Phys. Rept. **516** (2012) 1 [arXiv:1106.0034 [hep-ph]].
- [12] J.F. Gunion, H. Haber, G. Kane and S. Dawson, “*The Higgs Hunter’s Guide*”, Perseus Books, 1990.
- [13] S. L. Glashow and S. Weinberg, Phys. Rev. D **15** (1977) 1958.
- [14] S. L. Glashow and S. Weinberg, Phys. Rev. D **15** (1977) 1958; E. A. Paschos, Phys. Rev. D **15** (1977) 1966.
- [15] M. Aoki, S. Kanemura, K. Tsumura and K. Yagyu, Phys. Rev. D **80** (2009) 015017 [arXiv:0902.4665 [hep-ph]].

-
- [16] S. Davidson and H.E. Haber, Phys. Rev. **D72**, 035004 (2005); Erratum-ibid. **D72**, 099902 (2005); I.F. Ginzburg and M. Krawczyk, Phys. Rev. **D72**, 115013 (2005). F.J. Botella and J.P. Silva, Phys. Rev. **D51**, 3870 (1995).
- [17] Y. L. Wu and L. Wolfenstein, Phys. Rev. Lett. **73** (1994) 1762 [hep-ph/9409421].
- [18] F. J. Botella and J. P. Silva, Phys. Rev. D **51** (1995) 3870 [hep-ph/9411288].
- [19] C. C. Nishi, Phys. Rev. D **74** (2006) 036003 [Erratum-ibid. D **76** (2007) 119901] [hep-ph/0605153].
- [20] P. M. Ferreira, R. Santos and A. Barroso, Phys. Lett. B **603** (2004) 219 [Erratum-ibid. B **629** (2005) 114] [hep-ph/0406231].
- [21] A. Barroso, P. M. Ferreira and R. Santos, Phys. Lett. B **632** (2006) 684 [hep-ph/0507224].
- [22] A. Barroso, P. M. Ferreira, R. Santos and J. P. Silva, Phys. Rev. D **74** (2006) 085016 [hep-ph/0608282].
- [23] I. P. Ivanov, Phys. Rev. D **77** (2008) 015017 [arXiv:0710.3490 [hep-ph]].
- [24] P. Bechtle, O. Brein, S. Heinemeyer, G. Weiglein and K. E. Williams, Comput. Phys. Commun. **181** (2010) 138 [arXiv:0811.4169 [hep-ph]].
- [25] P. Bechtle, O. Brein, S. Heinemeyer, G. Weiglein and K. E. Williams, Comput. Phys. Commun. **182** (2011) 182 [arXiv:1102.1898 [hep-ph]].
- [26] P. Bechtle, O. Brein, S. Heinemeyer, O. Stål, T. Stefaniak et al., Eur. Phys. J C **74** (2014) 2693 [arXiv:1311.0055 [hep-ph]].
- [27] P. Bechtle, S. Heinemeyer, O. Stål, T. Stefaniak and G. Weiglein, Eur. Phys. J C **74** (2014) 2711 [arXiv:1305.1933 [hep-ph]].
- [28] R. V. Harlander, S. Liebler and H. Mantler, Comp. Phys. Commun. **184** (2013) 1605 [arXiv:1212.3249 [hep-ph]].
- [29] A. Djouadi, M. Spira and P.M. Zerwas, Phys. Lett. B **264** (1991) 440 and Z. Phys. C **70** (1996) 427; M. Spira *et al.*, Nucl. Phys. B **453** (1995) 17; A. Djouadi, J. Kalinowski and M. Spira, Comput. Phys. Commun. **108** (1998) 56; J. M. Butterworth, A. Arbey, L. Basso, S. Belov, A. Bharucha, F. Braam, A. Buckley and M. Campanelli *et al.*, arXiv:1003.1643 [hep-ph].
- [30] F. Mahmoudi, Comput. Phys. Commun. **178** (2008) 745 [arXiv:0710.2067 [hep-ph]]; F. Mahmoudi, Comput. Phys. Commun. **180** (2009) 1579 [arXiv:0808.3144 [hep-ph]].
- [31] R. Coimbra, M. O. P. Sampaio and R. Santos, Eur. Phys. J. C **73** (2013) 2428 [arXiv:1301.2599].
- [32] P. M. Ferreira, J. F. Gunion, H. E. Haber and R. Santos, Phys. Rev. D **89** (2014) 115003 [arXiv:1403.4736 [hep-ph]]; P. M. Ferreira, R. Guedes, M. O. P. Sampaio and R. Santos, arXiv:1409.6723 [hep-ph].

-
- [33] R. Contino, Y. Nomura and A. Pomarol, Nucl. Phys. B **671** (2003) 148 [hep-ph/0306259].
- [34] K. Agashe, R. Contino and A. Pomarol, Nucl. Phys. B **719** (2005) 165 [hep-ph/0412089].
- [35] R. Contino, L. Da Rold and A. Pomarol, Phys. Rev. D **75** (2007) 055014 [hep-ph/0612048].